Supporting Information: "Are Current Molecular Dynamics Force Fields too Helical?"

Robert B. Best,[1] Nicolae-Viorel Buchete[2] and Gerhard Hummer

Laboratory of Chemical Physics, National Institute of Diabetes and Digestive and Kidney Diseases, National Institutes of Health, Bethesda, MD 20892-0520; [1]current address: Department of Chemistry, Lensfield Road, Cambridge CB2 1EW, U.K.; [2]current address: School of Physics, University College Dublin, Belfield, Dublin 4, Ireland

E-mail: hummer@helix.nih.gov

Simulation Details

All simulations of Ala_5 were done in explicit TIP3P (1) solvent with periodic boundary conditions at constant pressure (1 atm) and temperature 300 K. A cubic simulation cell of initial side 32 Å was used, with electrostatics treated with particle mesh Ewald. Holonomic constraints (LINCS (2) in GROMACS (3,4) 3.3 and SETTLE (5) in NAMD2 (6)) were used to keep bonds to hydrogen atoms fixed and an integration time step of 2 fs was used. Simulations with the CHARMM27 (7,8) force field were run with NAMD2 (6) and all others with GROMACS (3,4) 3.3, using the GROMACS ports by Sorin and Pande for the Amber force fields (9). The amount of each simulation time for each force field can be found in Supporting Table S1; other details of simulation protocols have been published (10). The convergence of the calculated *J*-couplings over the simulations was assessed by plotting the average as a function of accumulated simulation time (Figure S2). Peptides with protonated C-termini carried a charge of +1 and were simulated both with and without counter-ions. In simulations of blocked peptides, the N-termini were acetylated, and the C-termini were capped by N-methylamide groups (Ace-Ala_5-NHMe).

Karplus Equation Parameters

The parameters (11,12) in Tables S1 to S3 refer to a Karplus equation of the form:

$$J(\theta) = A\cos^2(\theta+\Delta) + B\cos(\theta+\Delta) + C \qquad \textbf{(1)}$$

The following relation was used throughout this work to calculate $J_{\mathrm{HN}C\alpha}$ (in units of Hz) (12):

$$\begin{aligned} J_{\mathrm{HN}C\alpha}(\phi_i,\psi_{i-1}) = {} & -0.23\cos\phi_i - 0.20\cos\psi_{i-1} + 0.07\sin\phi_i \\ & +0.08\sin\psi_{i-1} + 0.07\cos\phi_i\cos\psi_{i-1} + 0.12\cos\phi_i\sin\psi_{i-1} \\ & -0.08\sin\phi_i\cos\psi_{i-1} - 0.14\sin\phi_i\sin\psi_{i-1} + 0.54 \end{aligned} \qquad \textbf{(2)}$$

Table S1: "Original" parameters used in Karplus equations by Graf *et al*. (12)

Coupling	Torsion	A (Hz)	B (Hz)	C (Hz)	Δ
$^3J_{HNH\alpha}$	ϕ_i	7.09	-1.42	1.55	-60°
$^3J_{HNC'}$	ϕ_i	4.29	-1.01	0.0	180°
$^3J_{H\alpha C'}$	ϕ_i	3.72	-2.18	1.28	120°
$^3J_{CC'}$	ϕ_i	1.36	-0.93	0.60	0°
$^3J_{HNC\beta}$	ϕ_i	3.06	-0.74	0.13	60°
$^1J_{NC\alpha}$	ψ_i	1.70	-0.98	9.51	0°
$^2J_{NC\alpha}$	ψ_{i-1}	-0.66	-1.52	7.85	0°

Table S2: "DFT1" parameters of Case and Brüschweiler (11). Where not listed, parameters are the same as in Table 1.

Coupling	Torsion	A (Hz)	B (Hz)	C (Hz)	Δ
$^3J_{HNH\alpha}$	ϕ_i	9.44	-1.53	-0.07	-60°
$^3J_{HNC'}$	ϕ_i	5.58	-1.06	-0.30	180°
$^3J_{H\alpha C'}$	ϕ_i	4.38	-1.87	0.56	120°
$^3J_{CC'}$	ϕ_i	2.39	-1.25	0.26	0°
$^3J_{HNC\beta}$	ϕ_i	5.15	0.01	-0.32	60°

Table S3: "DFT2" parameters of Case and Brüschweiler (11). Where not listed, parameters are the same as in Table 1.

Coupling	Torsion	A (Hz)	B (Hz)	C (Hz)	Δ
$^3J_{HNH\alpha}$	ϕ_i	9.14	-2.28	-0.29	-64.51°
$^3J_{HNC'}$	ϕ_i	5.34	-1.46	-0.29	172.49°
$^3J_{H\alpha C'}$	ϕ_i	4.77	-1.85	0.49	118.61°
$^3J_{CC'}$	ϕ_i	2.71	-0.91	0.21	-2.56°
$^3J_{HNC\beta}$	ϕ_i	4.58	-0.36	-0.31	58.18°

Table S4: Estimates of the errors σ_j of scalar couplings calculated using the Karplus equations are the root-mean-square deviations of experimental and calculated *J*-couplings from parameter fitting, either as explicitly given in Ref. (13), or as calculated from the experimental *J*-couplings given in the original publications (14,15). Note that since the same data were used in the fit, the σ_j may underestimate the real error. In addition, the values reported by Hu and Bax (13) correspond to mean absolute deviations rather than to root-mean-square deviations and therefore underestimate σ_j by 10-20% according to the authors' estimate. The same errors were assumed for all Karplus relations ("original", DFT1, and DFT2).

Coupling	σ_j (Hz)	Source
$^3J_{HNH\alpha}$	0.70	Hu and Bax (13)
$^3J_{HNC'}$	0.45	Hu and Bax (13)
$^3J_{H\alpha C'}$	0.29	Hu and Bax (13)
$^3J_{CC'}$	0.17	Hu and Bax (13)
$^3J_{HNC\beta}$	0.30	Hu and Bax (13)
$^1J_{NC\alpha}$	0.59	Ding and Gronenborn (14)
$^2J_{NC\alpha}$	0.50	Ding and Gronenborn (14)
$^3J_{HNC\alpha}$	0.10	Hennig *et al.* (15)

Table S5: Populations of α and β regions of the Ramachandran map before and after reweighting. The total simulation time for each force-field is given in ns. Reweighted populations in parentheses correspond to cases of very low β population before reweighting, and these data are not plotted in Figure 1 in the main text. Force-fields with unweighted χ^2 less than 2.25 for all the Karplus equation parameter sets are emphasized (bold, red). Literature references are given alongside the name of each force field.

			Unweighted		Reweighted					
					DFT1		DFT2		Orig	
FORCE-FIELD	terminus	Total sim. time (ns)	%α	%β	%α	%β	%α	%β	%α	%β
Amber03 (16)	blocked	400	62.3	15.9	7.2	51.6	5.1	33.8	3.2	13.6
Amber03 (16)	**zwitterionic**	**200**	**28.2**	**34.5**	**10.9**	**41.2**	**7.8**	**25.5**	**6.3**	**5.5**
Amber03 (16)	**protd c-ter**	**120**	**34.0**	**30.2**	**8.1**	**40.4**	**8.3**	**24.1**	**6.7**	**5.2**
Amber03 (16)	**prot c-ter, ions**	**120**	**33.0**	**30.7**	**11.0**	**39.9**	**8.0**	**24.5**	**6.6**	**5.3**
Amber99SB (17)	blocked	200	23.1	53.9	9.3	26.8	9.3	26.8	9.3	26.8
Amber99SB (17)	zwitterionic	200	19.2	56.2	17.9	26.2	14.5	14.8	7.6	5.4
Amber99SB (17)	protonated c-ter	120	19.9	55.7	16.0	26.8	12.7	17.8	6.9	6.6
Amber99SB (17)	prot c-ter, ions	120	19.7	55.5	14.4	31.0	11.7	18.3	7.3	6.9
Amber96 (18)	blocked	200	10.1	47.0	4.8	44.7	3.2	31.6	2.7	14.9
Amber96 (18)	prot c-ter, ions	80	10.5	46.8	8.9	34.2	8.6	22.7	4.5	7.3
Amber94 (19)	blocked	200	97.6	0.7	(61.2)	(21.5)	(61.5)	(16.1)	(61.8)	(11.2)
Amber94 (19)	prot c-ter, ions	80	90.1	2.5	(28.6)	(32.6)	(18.2)	(20.7)	(10.6)	(5.1)
Amber99 (20)	blocked	200	94.2	3.2	(63.8)	(32.8)	(63.5)	(30.7)	(61.0)	(38.0)
Amber99 (20)	prot c-ter, ions	80	89.9	6.8	(14.5)	(30.8)	(18.1)	(21.5)	(16.5)	(23.4)
Amber99p (9)	blocked	200	97.9	0.5	(72.7)	(15.3)	(80.2)	(12.0)	(84.8)	(8.2)
Amber99p (9)	prot c-ter, ions	80	93.6	2.1	(28.7)	(28.4)	(18.3)	(18.5)	(10.6)	(7.1)
AmberGSs (21)	blocked	1000	86.5	2.4	27.9	38.6	12.4	22.7	3.3	9.7
AmberGSs (21)	prot c-ter, ions	80	37.8	10.1	2.8	47.7	2.7	34.6	2.7	16.9
AmberGS (22)	blocked	200	79.0	3.7	2.4	51.9	2.4	37.7	2.3	21.3
AmberGS (22,23)	prot c-ter, ions	80	45.8	9.8	3.2	47.5	4.2	32.6	3.7	14.8
CHARMM27/cmap (7,8)	**prot c-ter, ions**	**80**	**41.5**	**25.3**	**14.0**	**32.1**	**14.1**	**18.7**	**11.4**	**7.1**
CHARMM27/cmap (7,8)	blocked	100	57.5	19.8	15.1	40.7	7.4	25.3	3.6	11.4
OPLS-aa/L (23)	blocked	400	32.8	32.0	3.4	52.3	3.1	29.3	2.4	7.8
OPLS-aa/L (23)	**prot c-ter, ions**	**80**	**30.9**	**33.5**	**10.0**	**42.0**	**7.7**	**22.3**	**5.2**	**3.9**
Gromos53a6 (24)	blocked	200	13.1	51.3	2.1	43.3	1.9	26.4	1.9	10.1
Gromos53a6 (24)	prot c-ter, ions	80	13.5	50.2	3.4	41.6	3.1	21.3	2.5	5.3
Gromos43a1 (25)	**prot c-ter, ions**	**80**	**14.0**	**41.2**	**2.4**	**40.8**	**2.3**	**23.7**	**2.6**	**8.6**

Table S6. χ^2 values with respect to the experimental data before and after reweighting. The reweighting energies ε_α and ε_β are given in units of k_BT. Force-fields with unweighted $\chi^2 \leq 2.25$ for all the Karplus equation parameter sets are emphasized (bold, red).

		Unweighted			Reweighted								
		χ^2			ORIGINAL			DFT1			DFT2		
Force field	**Terminus type**	**ORIG**	**DFT2**	**DFT1**	χ^2	ε_α	ε_β	χ^2	ε_α	ε_β	χ^2	ε_α	ε_β
Amber03	blocked	3.6	4.0	5.5	0.6	2.8	1.4	1.3	1.6	-0.6	0.9	2.2	0.2
Amber03	**zwitterionic**	**1.6**	**1.4**	**1.6**	**0.4**	**2.2**	**2.6**	**1.4**	**1.2**	**0.0**	**0.8**	**1.8**	**0.8**
Amber03	**prot c-ter**	**1.6**	**1.5**	**1.9**	**0.4**	**2.2**	**2.6**	**1.4**	**1.6**	**0.0**	**0.8**	**1.8**	**0.8**
Amber03	**prot c-ter, ions**	**1.6**	**1.5**	**1.8**	**0.3**	**2.4**	**2.6**	**1.4**	**1.4**	**0.0**	**0.8**	**2.0**	**0.8**
Amber99SB	blocked	6.2	6.2	6.2	1.6	1.8	1.8	1.6	1.8	1.8	1.6	1.8	1.8
Amber99SB	zwitterionic	4.3	5.2	4.4	0.6	2.0	3.6	1.6	0.8	1.6	1.0	1.2	2.4
Amber99SB	protonated c-ter	4.4	5.2	4.4	0.6	2.2	3.4	1.6	1.0	1.6	1.0	1.4	2.2
Amber99SB	prot c-ter, ions	4.2	4.9	4.2	0.6	2.0	3.4	1.7	1.0	1.4	1.0	1.4	2.2
Amber96	blocked	2.8	2.3	2.0	0.9	1.8	1.8	2.0	0.8	0.2	1.3	1.4	0.8
Amber96	prot c-ter, ions	2.3	2.2	1.9	0.4	1.4	2.6	1.6	0.4	0.6	0.9	0.6	1.2
Amber94	blocked	8.0	9.4	12.4	4.8	4.8	-0.4	6.5	4.8	-1.6	5.2	4.8	-1.0
Amber94	prot c-ter, ions	5.5	6.6	8.6	0.6	3.6	1.8	2.4	2.0	-1.0	1.4	2.8	0.0
Amber99	blocked	8.2	8.0	7.5	6.7	2.2	-3.4	6.6	2.2	-2.0	7.2	2.8	-1.4
Amber99	prot c-ter, ions	7.4	8.1	8.0	2.3	4.8	2.8	3.1	4.4	1.8	2.6	4.8	3.0
Amber99p	blocked	8.0	9.7	13.8	7.3	1.0	-1.6	8.2	1.4	-1.8	7.5	1.0	-2.0
Amber99p	prot c-ter, ions	6.0	6.8	8.8	0.8	4.6	-0.2	2.7	3.6	-1.2	1.5	4.4	-1.0
AmberGS(pande)	blocked	7.3	9.5	13.2	1.0	3.8	0.6	2.9	0.6	-4.4	2.0	2.0	-1.0
AmberGS(pande)	prot c-ter, ions	1.7	2.7	5.2	0.6	3.6	0.2	1.4	3.2	-1.4	0.9	3.2	-0.8
AmberGS	blocked	6.6	8.6	12.2	0.9	3.2	-0.4	1.4	2.8	-2.6	1.0	3.0	-1.4
AmberGS	prot c-ter, ions	1.9	2.8	5.2	0.7	2.8	-0.2	1.5	2.4	-1.8	1.0	2.6	-1.2
CHARMM27/cmap	**prot c-ter, ions**	**2.2**	**2.0**	**2.0**	**0.9**	**2.2**	**2.2**	**1.3**	**1.6**	**0.2**	**1.0**	**1.8**	**1.0**
CHARMM27/cmap	blocked	3.1	3.2	3.8	0.6	3.6	1.6	1.6	1.8	-0.2	1.1	2.8	0.6
OPLS-aa/L	blocked	2.2	2.3	2.3	0.5	3.2	2.2	1.4	2.4	-0.4	1.1	2.8	0.6
OPLS-aa/L	**prot c-ter, ions**	**2.0**	**2.0**	**1.8**	**0.4**	**2.8**	**3.0**	**1.5**	**1.6**	**0.0**	**1.1**	**2.2**	**1.0**
Gromos53a6	blocked	2.3	2.3	1.8	0.6	2.8	2.6	1.4	2.2	0.6	1.0	2.6	1.4
Gromos53a6	prot c-ter, ions	2.3	2.3	1.8	0.4	2.6	3.2	1.4	1.8	0.6	0.9	2.2	1.6
Gromos43a1	**prot c-ter, ions**	**1.6**	**1.4**	**1.4**	**0.5**	**2.2**	**2.2**	**1.2**	**2.0**	**0.2**	**0.7**	**2.2**	**1.0**

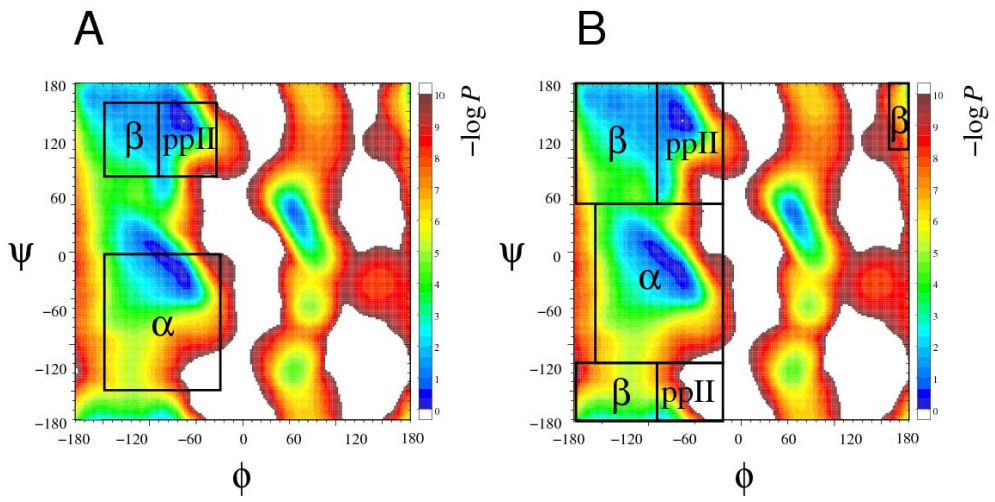

Figure S1. Definitions of the three main regions of Ramachadran space used in (A) Graf *et al.* (12) and (B) in the present work, superimposed on –log $P(\phi,\psi)$, where $P(\phi,\psi)$ is the probability density of backbone (ϕ,ψ) angles from a PDB-derived database (26), excluding glycine and proline and residues in segments of defined secondary structure. Note that the populations of the minima in this data set are not expected to be quantitatively representative of unstructured peptides in solution.

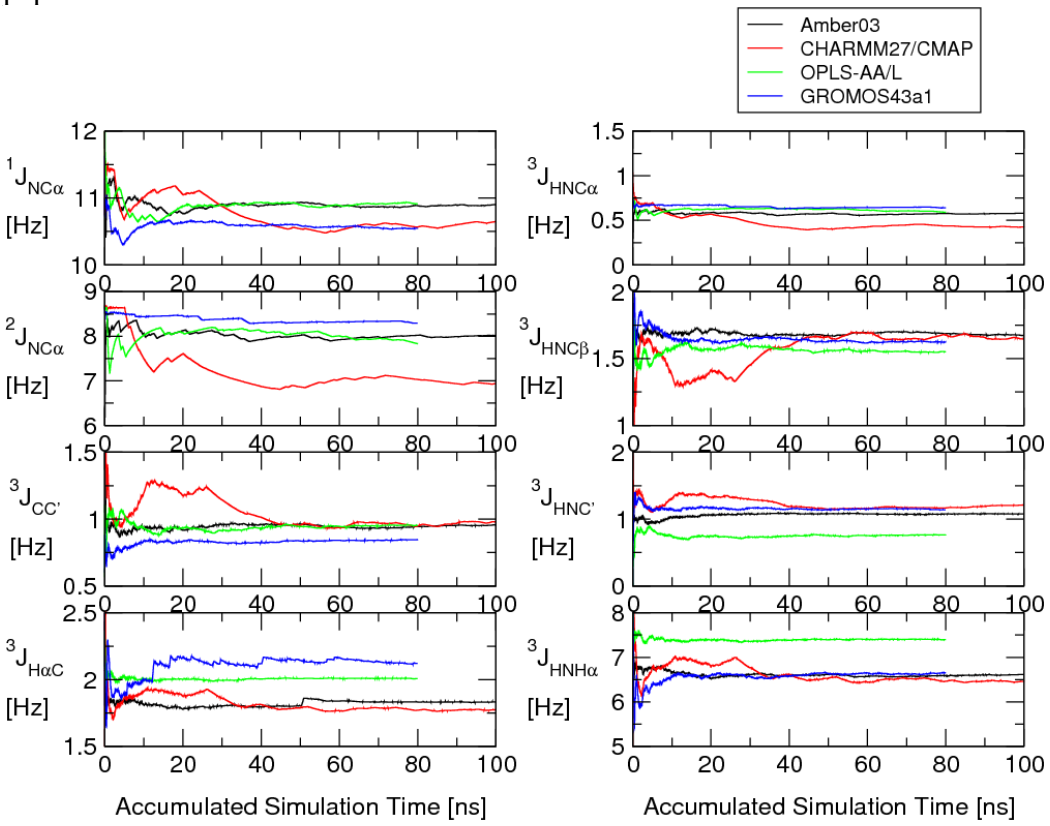

Figure S2. Convergence of calculated couplings as a function of the accumulated simulation time. Average couplings, shown here for residue 3, were calculated using the original set of Karplus parameters of Graf *et al.* (12) for four force-fields. In all cases the peptides were unblocked and protonated, except for CHARMM in which the blocked form was used.

References

1. Jorgensen, W. L., J. Chandrasekhar, and J. D. Madura. 1983. Comparison of simple potential functions for simulating liquid water. J. Chem. Phys. 79:926-935.
2. Hess, B., H. Bekker, H. J. C. Berendsen, and J. G. E. M. Fraaije. 1997. LINCS: a linear constraint solver for molecular simulations. J. Comp. Chem. 18:1463-1472.
3. Van der Spoel, D., E. Lindahl, B. Hess, G. Groenhof, A. E. Mark, and H. J. C. Berendsen. 2005. GROMACS: Fast, Flexible and Free. J. Comp. Chem. 26:1701-1718.
4. Lindahl, E., B. Hess, and D. van der Spoel. 2001. GROMACS 3.0: a package for molecular simulation and trajectory analysis J. Mol. Model. 7:306-317.
5. Miyamoto, S. and P. A. Kollman. 1992. Settle - an analytical version of the shake and rattle algorithm for rigid water models. J. Comp. Chem. 13:952-962.
6. Phillips, J. C., R. Braun, W. Wang, J. Gumbart, E. Tajkhorshid, E. Villa, C. Chipot, R. D. Skeel, K. Laxmikant, and K. Schulten. 2005. Scalable molecular dynamics with NAMD. J. Comp. Chem. 26:1781-1802.
7. MacKerell, A. D., D. Bashford, M. Bellot, J. R. L. Dunbrack, J. D. Evanseck, M. J. Field, S. Fischer, J. Gao, H. Guo, S. Ha, D. Joseph-McCarthy, L. Kuchnir, K. Kuczera, F. T. K. Lau, C. Mattos, S. Michnick, T. Ngo, D. T. Nguyen, B. Prodhom, W. E. Reiher, III, B. Roux, M. Schlenkrich, J. C. Smith, R. Stote, J. Straub, M. Watanabe, J. Kuczera, D. Yin, and M. Karplus. 2000. All-atom empirical potential for molecular modeling and dynamics studies of proteins. J. Phys. Chem. B 102:3586-3616.
8. MacKerell, A. D., M. Feig, and C. L. Brooks. 2004. Improved treatment of the protein backbone in empirical force fields. J. Am. Chem. Soc. 126:698-699.
9. Sorin, E. J. and V. S. Pande. 2005. Exploring the helix-coil transition via all-atom equilibrium ensemble simulations Biophys. J. 88:2472-2493.
10. Buchete, N.-V. and G. Hummer. 2008. Coarse-grained master equations for peptide folding kinetics from atomistic molecular simulations. J. Phys. Chem. B 112:6057-6069.
11. Case, D. A., C. Scheurer, and R. Brüschweiler. 2000. Static and dynamic effects on vicinal scalar *J* couplings in proteins and peptides: a MD/DFT analysis. J. Am. Chem. Soc. 122:10390-10397.
12. Graf, P. H. Nguyen, G. Stock, and H. Schwalbe. 2007. Structure and dynamics of the homologous series of alanine peptides: a joint molecular dynamics/NMR study. J. Am. Chem. Soc. 129:1179-1189.
13. Hu, J.-S. and A. Bax. 1997. Determination of ϕ and χ_1 angles in proteins from ^{13}C-^{13}C three-bond *J* couplings measured by three-dimensional heteronuclear NMR. How planar is the peptide bond? J. Am. Chem. Soc. 119:6360-6368.
14. Ding, K. and A. M. Gronenborn. 2004. Protein backbone ^{1}HN-$^{13}C\alpha$ and ^{15}N-$^{13}C\alpha$ residual dipolar and *J* couplings: new constraints for NMR structure determination. J. Am. Chem. Soc. 126:6232-6233.
15. Hennig, M., W. Bermel, H. Schwalbe, and C. Griesinger. 2000. Determination of psi torsion angle restraints from $^{3}J_{C\alpha C\alpha}$ and $^{3}J_{C\alpha HN}$ coupling constants in proteins. J. Am. Chem. Soc. 122:6268-6277.
16. Duan, Y., C. Wu, S. Chowdhury, M. C. Lee, G. Xiong, W. Zhang, R. Yang, P. Cieplak, R. Luo, T. Lee, J. Caldwell, J. Wang, and P. A. Kollman. 2003. A point-charge force field for molecular mechanics simulations of proteins based on condensed-phase quantum chemical calculations. J. Comp. Chem. 24:1999-2012.

17. Hornak, V., R. Abel, A. Okur, B. Strockbine, A. Roitberg, and C. Simmerling. 2006. Comparison of multiple AMBER force-fields and development of improved protein backbone parameters. Proteins 65:712-725.
18. Kollman, P. A. 1996. Advances and continuing challenges in achieving realistic and predictive simulations of the properties of organic and biological molecules. Acc. Chem. Res. 29:461-469.
19. Cornell, W. D., P. Cieplak, C. I. Bayly, I. R. Gould, K. M. Merz, D. M. Ferguson, D. C. Spellmeyer, T. Fox, J. W. Caldwell, and P. A. Kollman. 1995. A second generation force field for the simulation of proteins, nucleic acids and organic molecules. J. Am. Chem. Soc. 117:5179-5197.
20. Wang, J., P. Cieplak, and P. A. Kollman. 2000. How well does a restrained electrostatic potential (RESP) model perform in calculating conformational energies of organic and biological molecules? J. Comp. Chem. 21:1049-1074.
21. Nymeyer, H. and A. E. Garcia. 2003. Proc. Natl. Acad. Sci. U. S. A. 100:13934-13939.
22. García, A. E. and K. Y. Sanbonmatsu. 2002. α-Helical stabilization by side chain shielding of backbone hydrogen bonds. Proc. Natl. Acad. Sci. U. S. A. 99:2782-2787.
23. Kaminski, G. A., R. A. Friesner, J. Tirado-Rives, and W. L. Jorgensen. 2001. Evaluation and reparameterization of the OPLS-AA force field for proteins via comparison with accurate quantum chemical calculations on peptides. J. Phys. Chem. B 105:6474-6487.
24. Oosterbrink, C., A. Villa, A. E. Mark, and W. F. Van Gunsteren. 2004. A biomolecular force-field based on the free enthalpy of hydration and solvation: the Gromos force-field parameter sets 53A5 and 53A6. J. Comp. Chem. 25:1656-1676.
25. Eising, A. A., P. H. Hünenberger, P. Krüger, A. E. Mark, W. R. P. Scott, and I. G. Tironi. 1996. Biomolecular simulation: the GROMOS96 manual and user guide. Zürich: Vdf Hochschulverlag, ETH Zürich.
26. Lovell, S. C., I. W. Davis, W. B. Arendall, P. I. W. de Bakker, J. M. Word, M. G. Prisant, J. S. Richardson, and D. C. Richardson. 2003. Structure validation by Cα geometry: φ,ψ and Cβ deviation. Proteins 50:437-450.